TÜBİTAK

Turkish Journal of Earth Sciences

http://journals.tubitak.gov.tr/earth/

Research Article

Turkish J Earth Sci
(2023) 32: 961-974

doi:10.55730/1300-0985.1886

The petrogenesis of analcime in the Coppermine Formation on Robert Island, South Shetland Islands, Antarctica

Raif KANDEMİR[1], Yılmaz DEMİR[1], Cüneyt ŞEN[2,*], Ufuk Celal YAĞCIOĞLU[2]

[1]Department of Geological Engineering, Engineering Faculty, Recep Tayyip Erdoğan University, Rize, Turkiye
[2]Department of Geological Engineering, Engineering Faculty, Karadeniz Technical University, Trabzon, Turkiye

Received: 30.04.2023 • **Accepted/Published Online:** 17.11.2023 • **Final Version:** 28.11.2023

Abstract: The South Shetland Islands were shaped by island arc volcanism that occurred from the Jurassic to the Quaternary. Robert Island is located in the center of this archipelago, and Coppermine Peninsula, located on the southwestern part of Robert Island, exposures significant rock outcrops of basalts and andesitic-basaltic agglomerates of the Coppermine Formation. The investigated samples were collected during Turkish Antarctic Expedition 2 (TAE-II), in March–April 2018, from the area northeast of Triplet Hill. The volcanic rocks exhibited an amygdaloidal microlithic-porphyritic texture. Subhedral to anhedral phenocrysts of labradorite, augite, and olivine were observed with holocrystalline groundmass composed of plagioclase, pyroxene, and opaques. Petrographic studies revealed that the vesicles were initially coated with clay minerals, and X-ray diffraction studies showed that mostly analcime and carbonates, and less amount of zeolites filled the vesicles. Herein, it was aimed to discuss the analcime formation. Fluid inclusion studies performed on the analcime revealed homogenization temperatures ranging from 83 to 268 °C. The eutectic temperatures of the fluid inclusions suggested that these minerals were formed from NaCl-dominated solutions that contained a limited amount of $MgCl_2$ and $CaCl_2$. The salinity of these inclusions ranged between 0.2–2.9 wt.% NaCl equivalent, and exhibited final ice melting temperatures of –1.7 to –0.1 °C. These salinity values, which are lower than the average salinity values of seawater, suggest that the formation of the analcime and the fibrous zeolites (thomsonite and stilbite) was closely associated with meteoric solutions. Consequently, the salinity values of the fluid inclusions suggest the mixing of meteoric waters form from glaciers and seawater at different rates.

Key words: Antarctica, South Shetland Islands, Robert Island, Coppermine Formation, vesicle fillings, analcime

1. Introduction

Amygdaloidal volcanic rocks are abundant in the Coppermine Formation on Robert Island, South Shetland Islands, located within the Antarctic Circle. The extreme alteration and infilling processes undergone by the rocks found in the polar regions are less well-known compared to other geographic areas. Indeed, a majority of the data on alteration and infilling processes in polar geological formations come from geothermal fields in Iceland (e.g., Kristmannsdottir, 1979; Weisenberger and Selbekk, 2010). Chipera and Apps (2001) observed that the distribution of secondary minerals varied as a function of temperature in hydrothermally altered Icelandic basalts. Hydrothermal fluids in these formations are channeled through permeable zones, with the various anionic and cationic complexes being formed either by precipitation in void spaces or by interactions with the wall rock. In all instances, the system will contain infills that are either partially or wholly derived from precipitation within the fluid-filled voids or from alteration reactions with the wall rocks (Triana et al., 2012). While common void-filling minerals are primarily composed of zeolite and various carbonate minerals below ~250 °C, minerals such as mixed-layered smectite/chlorite, chlorite, epidote, and prehnite are common at temperatures above 200 °C (Chipera and Apps, 2001).

Analcime is a common infilling mineral that is unique to basaltic rocks. Some researchers consider it to be a member of the feldspathoid group due to its similarity to their crystallographic structure; however, it is generally classified as a tectosilicate mineral in the zeolite group, as it contains molecular water in its crystal structure ($NaAlSi_2O_6 \cdot H_2O$). Analcime minerals are found in a variety geological environments, including 1) hydrothermal fractures in volcanic rocks as a result of secondary reactions (Keith et al., 1983; Bargar and Beeson, 1985); 2) transformation products from the exchange of K^+–Na^+ ions in leucite crystals formed in magmatic rocks with a high concentration of Na^+ in the solution (Putnis

* Correspondence: csen@ktu.edu.tr

et al., 1994); 3) crystallization in basic environments in paleo-lacustrine basins with high salinities (Gall and Hyde, 1989); 4) alteration resulting from the dissolution of volcaniclastic sediments, such as plagioclase and glass (Sheppard and Hay, 2001); 5) a result of burial or contact metamorphism in low-grade metamorphic regimes (Boles and Coombs, 1975); 6) diagenetic products of the partial burial of deep-sea sediments; and 7) primary crystallization in sodium-rich magmatic rocks (Pearce, 1970). Consequently, analcime crystals were specifically selected for the investigation of void-filling minerals in the basalts of the Coppermine Formation.

This study investigated the origin of analcime crystals formed under polar conditions in the vesicles of the volcanic rocks on Robert Island, one of the central islands of the South Shetland Islands in the Southern Antarctic Peninsula. The South Shetland Islands have been located near the polar circle for the last 90 million years (Poblete et al., 2011, and references therein). X-ray powder diffraction (XRD) and fluid inclusion studies were conducted to understand the alteration of volcanic host rock and infilling conditions that controlled the formation of void-filling analcime in the Coppermine Formation.

2. Geological setting

The South Shetlands Islands lie approximately 950 km southeast of Cape Horn and 100 km northwest of the Antarctica Peninsula and are located between the Drake Passage and the Bransfield Strait (Figure 1). The South Shetland Islands are comprised of about a dozen medium to large islands, with the largest being King George Island (~80 × 25 km); they also include hundreds of minor islands and offshore shoals (Haase et al., 2012). Robert Island, on which the study area is located, can be found

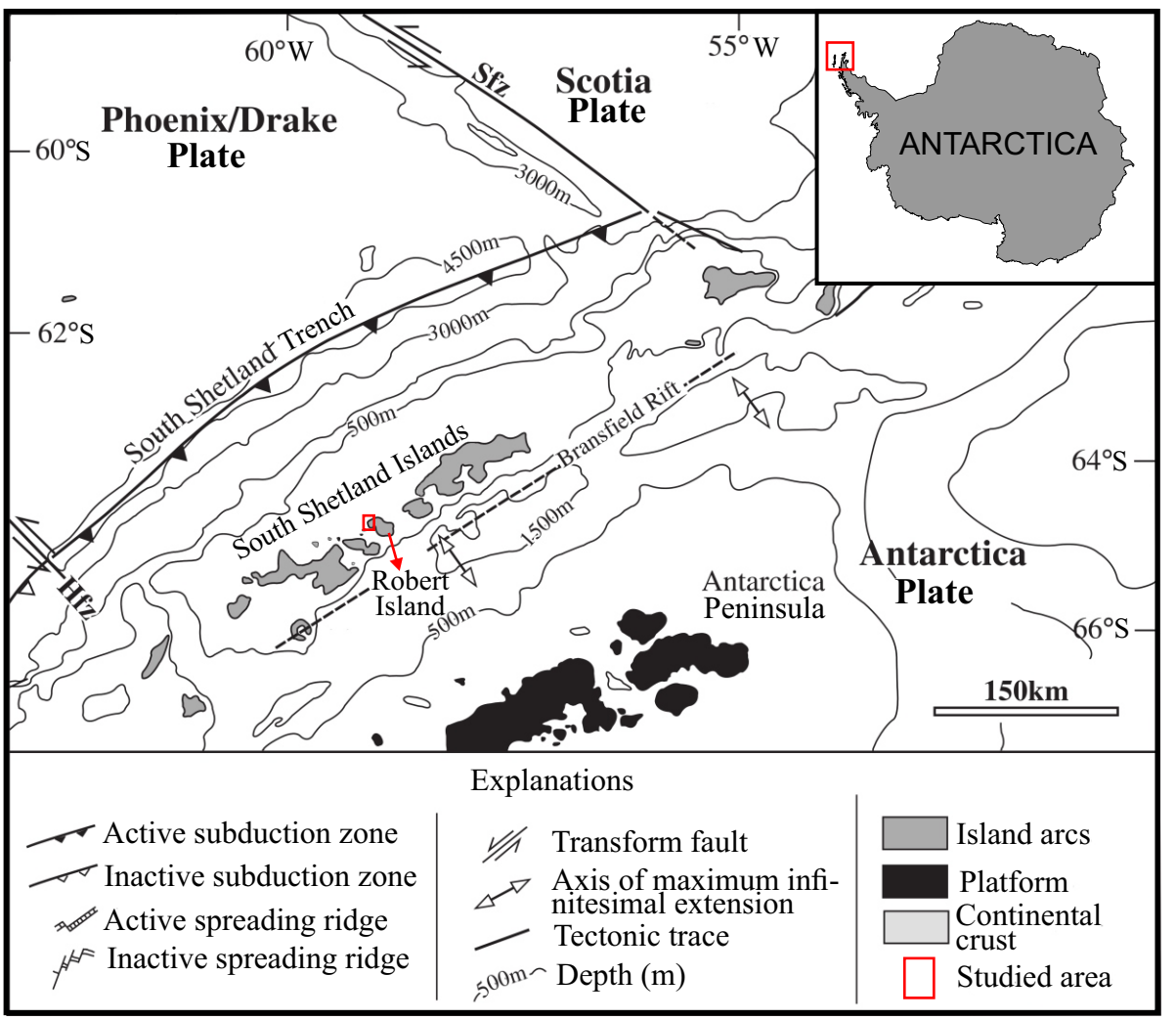

Figure 1. Tectonic setting of the South Shetland archipelago and Antarctica Peninsula. Sfz: Shackleton Fault Zone, SSR: South Scotia Ridge, Hfz: Hero Fault Zone (modified from Machado et al., 2005).

northwest of the Antarctic Peninsula (Figure 1). The South Shetland Islands were shaped by a period of island arc volcanism that occurred between the Jurassic and the Quaternary and sit on a sialic basement of schists and deformed sedimentary rocks (Smellie et al., 1984). The formation of the South Shetland Island arc began with the accumulation of the southwestern part of the archipelago during the Late Jurassic or Early Cretaceous. The largest islands in this volcanic archipelago are formed mainly of Mesozoic and Cenozoic volcanic rocks as well as associated volcanoclastic rocks (Smellie et al., 1984; Leat et al., 1995).

Robert Island (~18 × 18 km) is located in the central part of the archipelago and is mostly covered by a single ice cap. The largest outcrop on the island can be found on its southwest coast, on the Coppermine Peninsula. These rocks form part of the Coppermine Formation, which is dominated by basalts and andesitic-basaltic agglomerates (e.g., Hervé, 1965; González Ferran and Karsui, 1970; Smellie et al., 1984; Bastías et al., 2023). Smellie et al. (1984) showed that the K-Ar ages of the Coppermine Formation range from ~83–78 Ma. Villanueva (2021) reviewed the geology of the Coppermine Peninsula and reported $^{40}Ar/^{39}Ar$ plateau ages between ~81 and 62 Ma. Numerous gas cavities, ranging from millimeters to decimeters in size, were traced along with the grossly altered stratigraphic layers of the Coppermine Formation (Smellie et al., 1984). Aydar et al. (2019) reported tuya-like morphological structures that could be observed in the formation, formed by lava-fed delta products; these structures, together with breccias with pillow lava and hyaloclastites, are indicative of subglacial volcanism. They also classified the volcanic rocks into 2 main petrographic types, represented by the association of clinopyroxene + plagioclase ± olivine and clinopyroxene + orthopyroxene + plagioclase.

The Coppermine Formation is cut by Paleocene and Eocene-aged basaltic and basaltic andesite dikes (Kraus, 2005; Machado et al., 2005; Kamenov, 2008; Haase et al., 2012). Haase et al. (2012) suggested that these dykes were related to rifting and marginal (back-arc) basin formation behind the South Shetland Island arc.

3. Field sampling and analytical methods

Fieldwork was conducted as part of Turkish Antarctic Expedition 2 (TAE-II) in March–April 2018. The primary study area was located northeast of Triplet Hill (Figure 2), where a glacier-free outcrop of the Coppermine Peninsula was exposed. A total of 90 samples were collected during the expedition, of which 3 samples that exhibited significant amounts of void-infilling were selected and used in this study.

A Nikon-transmitted light microscope (Nikon Corp., Minato City, Tokyo, Japan) was used to observe the optical properties of the minerals in thin sections. These thin sections were prepared at the Departments of Geological Engineering of Karadeniz Technical University and Recep Tayyip Erdoğan University. XRD analysis of the very fine-grained secondary minerals in the voids of the rocks was performed using a Rigaku SmartLab (Rigaku Corp.,

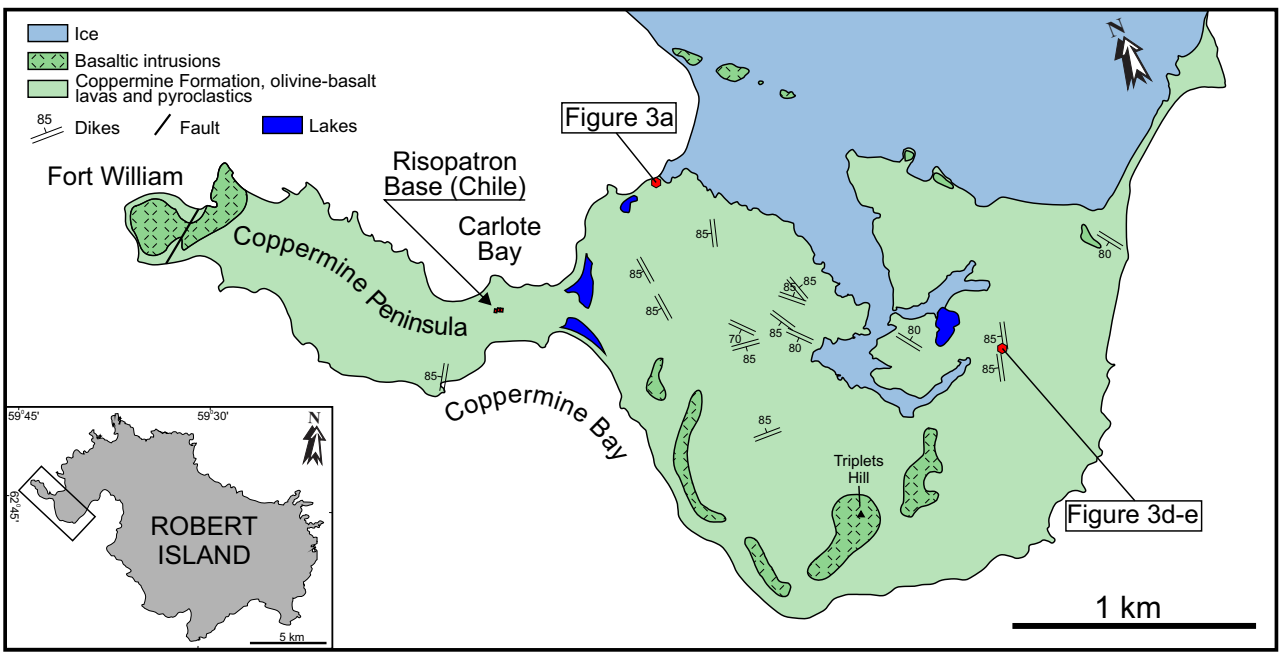

Figure 2. Geological map of the Coppermine Peninsula, Robert Island (modified from Smellie et al., 1984).

Tokyo, Japan) with a CuKα source and a step size of 0.02° between 5 and 70° at the Central Research Laboratory of Recep Tayyip Erdogan University.

Microthermometric measurements were conducted on approximately 200-μm of double-polished wafers using a Linkam THMG600 heating–freezing stage (Linkam Scientific Instruments Ltd., Salfords, Redhill, UK) mounted on an Olympus BX-51 microscope (Olympus Scientific Solutions, Shinjuku, Tokyo, Japan) at the Department of Geological Engineering of Recep Tayyip Erdogan University, Türkiye. This equipment is suitable for temperature measurements between −196 and 600 °C. Liquid nitrogen was used for the cooling and freezing processes. The heating and freezing stages were calibrated using H_2O- and H_2O–CO_2- containing synthetic fluid inclusions. Repeated experiments showed that the measurements were performed at an accuracy of ±0.2 °C and ±1 °C for the freezing and heating processes, respectively. Salinity data were expressed as wt.% NaCl equivalent and were calculated from the final melting temperature of the ice crystal (Tm-ice) using the equation reported by Bodnar (1993). A total of 3 double-polished wafers were prepared from the analcime samples. Prior to the microthermometric measurements, the fluid inclusions were petrographically investigated using the criteria described by Roedder (1984). The measurements were then conducted according to the procedure described by Shepherd et al. (1985).

4. Results

4.1. Field description and petrography of the volcanic rocks

The Coppermine Formation is composed of 5–7-m-thick basalt-andesite lava flows with intercalated pyroclastic rocks. Smellie et al. (1984) noted that these lava flows are relatively widespread and are characterized by prominent alternating pairs of parallel pale and dark brown bands, with the colors often corresponding to differences in hardness (Figure 3a). The contacts between the lava flows and the pyroclastic rocks are characterized by prominent, red-colored scoriaceous rocks (Figure 3b). The softer bands, which are often twice as thick as the harder bands, contain an abundance of voids that are filled by carbonates, clay minerals, and/or zeolite. This alteration is likely to be deuteric, with carbonate-, clay mineral-, and zeolite-filled amygdales occurring in the softer bands that are flanked by harder, less amygdaloidal bands (Figures 3b–3e). No significant mineralogical differences were observed between the 2 layers (Smellie et al., 1984).

The rocks exhibit hypabyssal and porphyritic textures, with the basalt exhibiting an amygdaloidal microlithic-porphyritic texture. Subhedral to anhedral phenocrysts of labradorite, augite, and olivine are observed in a coarse, holocrystalline groundmass composed of plagioclase, pyroxene, and opaques. Both the phenocrysts and holocrystalline groundmass exhibit signs of alteration. Sericite and clay minerals are commonly observed at the center of the concentrically zoned labradorites. The rims of the augites have been altered to chlorite, and the olivines are mostly serpentinized. There are many cases where the crystalline matrix has been replaced by zeolite, silica, carbonates, chlorite, and clay minerals. Carbonates were the most common alteration minerals, forming in the phenocrysts of plagioclase and pyroxene as well as in the groundmass.

Centimeter-scale amygdales were observed in various forms, including spherical, oval, and flattened morphologies. At least 4 different vesicle infillings were identified (Figure 4), comprising (Type 1) void walls completely clay minerals lined and carbonates filled inside the void; (Type 2) void wall clay minerals lines fragmented and mixed inside the void with carbonates; (Type 3) void walls clay and/or carbonate minerals lined and analcime filled inside the void; and (Type 4) carbonate mixed fragmented lines of clay minerals fill inside the void besides to analcimes. Analcime and zeolite were observed at the center of these voids. Vesicles smaller than 250 μm were often characterized by Type 1 and Type 2 infillings.

4.2. X-ray diffraction

Analcime, stilbite, thomsonite, and dolomite were identified from the X-ray diffractograms (Figures 5a–5d). Thomsonite was distinguishable by a characteristic peak at $2\theta = 9.2°$ with d = 9.30 Å (Figure 5a), while analcime crystals were distinguished by a characteristic peak at $2\theta = 26°$ with d = 3.43 Å (Figure 5a). Dolomites were identified by a characteristic peak at $2\theta = 31.04°$ with d = 2.88 Å (Figure 5b). Stilbite crystals are characterized by a peak at $2\theta = 9.7°$ with d = 9.13 Å (Figures 5c and 5d).

4.3. Fluid inclusion studies

4.3.1. Petrography

Fluid inclusion studies were conducted on the analcime crystals (Figure 6a) to determine the temperature during the formation of these minerals as well as the composition of the solutions during their formation. Prior to the microthermometric experiments, a genetic classification of the fluid inclusions in each crystal was performed according to the criteria proposed by Shepherd et al. (1985). Primary inclusions were observed to be isolated and aligned parallel to the host crystals (Figures 6b–6e), while secondary inclusions were observed to take the form of trails that occurred as planar groups or in fractures that cut the crystal boundaries. The primary inclusions were commonly isometric, rounded, polygonal, and tube-shaped; few irregular inclusions were observed. In contrast, the secondary inclusions commonly exhibited irregular morphologies (Figures 6f–6i). The size of the

Figure 3. Alternating lava flows of the Coppermine Formation cropping out at Triple Hill (a), contact between the hard parts and the soft parts of the formation, (b) filled vesicles in the soft parts (c), and hard parts of the formation (d and e).

primary inclusions ranged between 10 and 30 μm, while the secondary inclusions were larger, with sizes of up to 60 μm. The primary and secondary fluid inclusions did not coexist. None of the fluid inclusions contained halite or separated liquid CO_2 phases at room temperature. Both the primary and secondary inclusions were liquid-bearing 2-phase (L+V) inclusions, with vapor ratios ranging between 5 and 25 vol.%. Microthermometric measurements were carried out on both the primary and secondary inclusions. Both types of the inclusions were found to be homogenized to the liquid phases. The primary inclusions were characterized by their higher homogenization temperatures (Th) compared to the secondary inclusions. However, the salinity and eutectic temperatures (Te) of both types of fluid inclusions were relatively similar. The detailed microthermometric properties of each type of inclusion are described below.

4.3.2. Microthermometric measurements of analcime

The Te of the primary and secondary inclusions were measured, and the results are presented in the Table. The Te of the primary fluid inclusions ranged between –54.8 and –23.5 °C, while the secondary fluid inclusions exhibited similar Te, ranging between –45.6 and –21.9 °C (Figure 7a). The Te of the Type I inclusions were compared to various water–salt systems, and a majority of the inclusions exhibited Te that were similar to that of an H_2O–NaCl system (Hein, 1989). Other water–salt

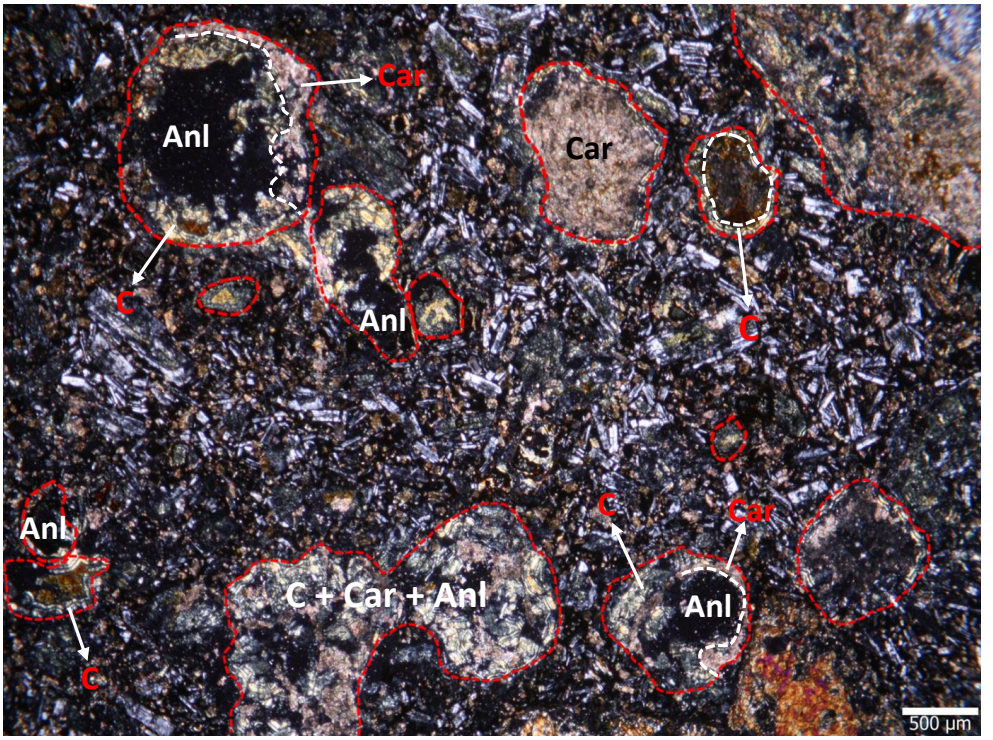

Figure 4. Microphotograph of the vesicles under cross Nicols (Anl-analcime, Car- carbonates, C- clay minerals).

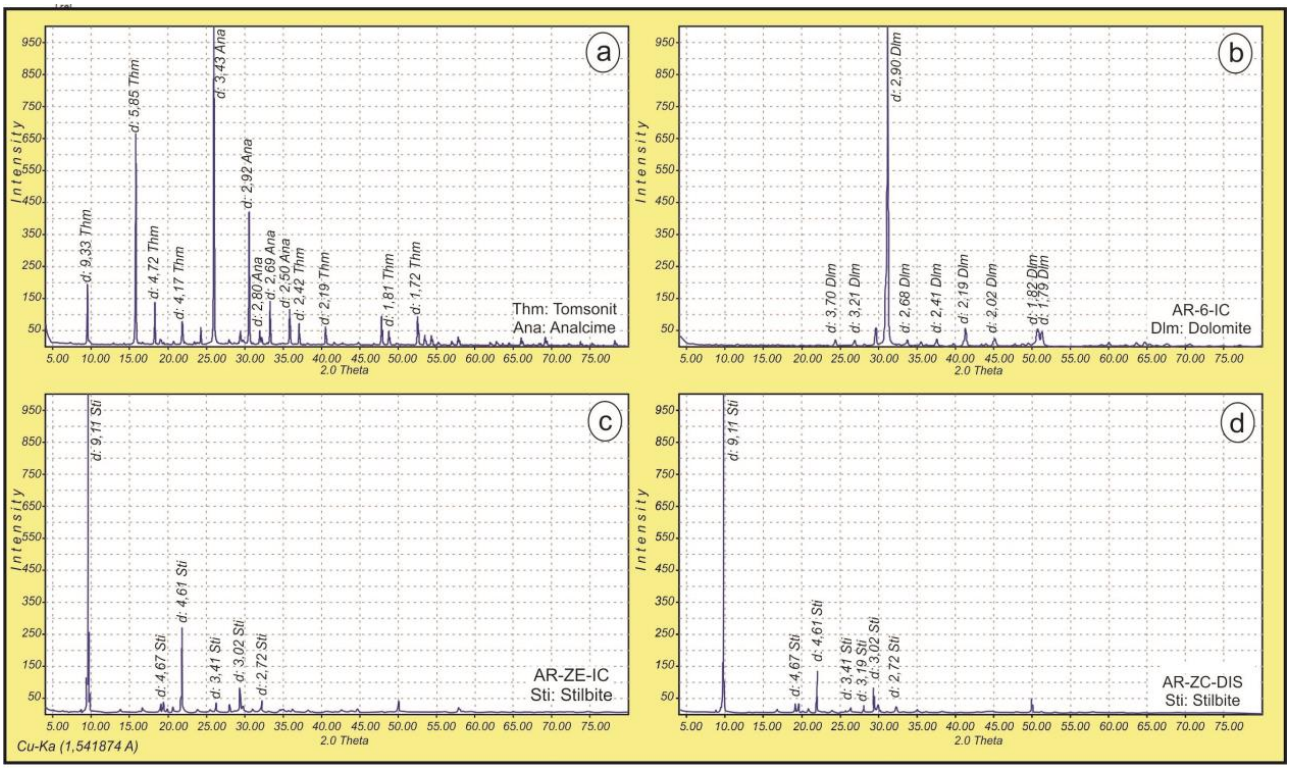

Figure 5. XRD diffractograms. Analcime and tomsonite (a), dolomite (b)

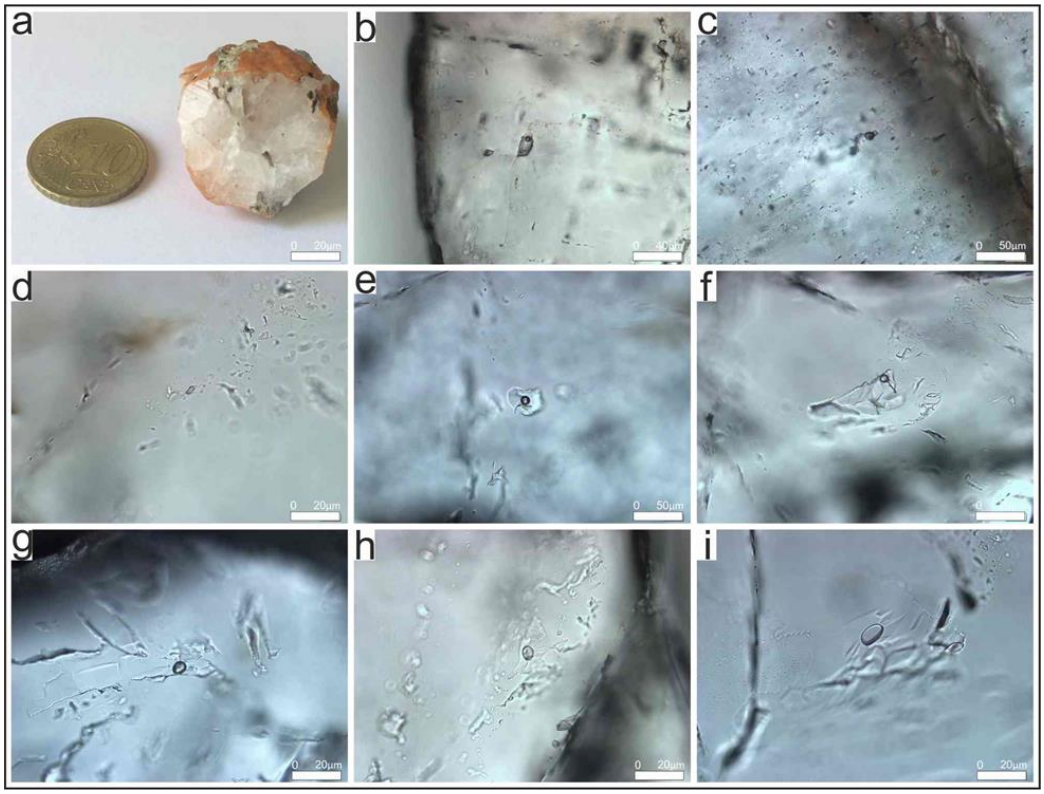

Figure 6. Macroscopic view of the vesicle filling sample (a), primary fluid inclusions (b–e), and secondary fluid inclusions (f–i) in the analcime.

systems that may have been present included the H_2O–$MgCl_2$ system (Te = –33.6 °C) and H_2O–$CaCl_2$-dominated solutions (Te = –49.8 °C).

The Tm-ice of the primary and secondary fluid inclusions were measured to determine their salinity (Table). The Tm-ice of the primary inclusions ranged between –0.4 and –1.7 °C, representing a salinity ranging between 0.7 and 2.9 wt.% NaCl equivalent (Bodnar, 1993). The Tm-ice of the secondary fluid inclusions were relatively similar, ranging between –0.1 and –1.6 °C, representing a salinity ranging between 0.2 and 2.7 wt.% NaCl equivalent. The calculated salinities of both types of inclusions were less than the average salinity of ocean water (Figure 7b), and there was no difference between the types of inclusions when plotted on a Th-salinity diagram (Figure 7b). However, the Th of these inclusions were relatively different, with the primary fluid inclusions exhibiting Th that ranged between 180 and 268 °C compared to the secondary inclusions, which exhibited Th ranging between 83 and 154 °C. The temperatures of both types of inclusions are represented by bimodal distributions on a Th histogram given in Figure 7c. In summary, the primary inclusions were characterized by their higher Th compared to the secondary inclusions, but the salinity and Te of both types of fluid inclusions were relatively similar.

5. Discussion

5.1. Vesiculation of the lava flows of the Coppermine Formation

In ocean arc volcanism, volatile content is determined by the quantity of the subducting hydrated oceanic plate as well as the assimilation and fractional crystallization behavior of the ascending mantle melt. Volcanic arc basalts typically have a greater volatile content than basalts from other tectonic environments. For example, studies on preprimitive arc basalts from the Izu-Bonin volcanic arc have found that olivine-hosted melt inclusions can contain up to 5% H_2O (Kuritani et al., 2014; Ushioda et al., 2014).

The volcanic rocks from the Coppermine Formation had low- to medium-potassium (0.34–1.00 wt.%, n = 12) tholeiitic to calc-alkaline transitional (MgO = 6.1–12.1 wt.%; Mg# = 0.65–0.77) basaltic volcanic rocks (Smellie et al., 1984). Field observations of the formation showed that the presence of decimeter-sized voids indicated that these rocks were formed from a volatile-rich arc magma.

The size, shape, concentration, and distribution of preserved vesicles in solidified lava flows are dependent on dynamic, thermal, and physicochemical processes that occur within the lava (Manga, 1996). The shapes of vesicles reflect the local strain rate (Stein and Spera, 1992; Stone, 1994), while the shape of the vesicles provides constraints

Table. Measured microthermometric parameters of the zeolites from the Coppermine Formation (P: primary fluid inclusions, S: secondary fluid inclusions, n.d.: not detected).

Sample	FI types	Eutectic (Te, °C)	Ice melting (Tm-ice, °C)	Salinity (wt% NaCl equ.)	Homogenization temp. (Th, °C)
1	S	–27	–1.6	2.7	122
		–28.5	–0.6	1.1	128
		–27.4	–0.3	0.5	127
		–25.6	–1.6	2.7	124
		–43	–1.3	2.2	128
		–31.7	–0.9	1.6	131
		–21.9	–0.7	1.2	140
	P	–26.3	–0.6	1.1	245
		n.d.	–1.4	2.4	258
		–25	–1.4	2.4	255
		–30.1	–0.6	1.1	268
		–23.7	–0.8	1.4	249
	S	–44.1	–0.8	1.4	83
		–28.4	–0.6	1.1	83
		–29.5	–0.1	0.2	112
2	S	–25.8	–0.3	0.5	141
	P	–32.5	–0.6	1.1	180
	S	–24.8	–1.1	1.9	147
		–39.6	–0.8	1.4	143
		–24.5	–0.6	1.1	154
		–31.1	–0.2	0.4	143
		–45.6	–0.7	1.2	144
		–25.3	–0.5	0.9	138
		–27.7	–0.4	0.7	138
		–37.6	–0.5	0.9	138
		n.d.	–0.6	1.1	119
		–30.5	–0.9	1.6	130
		–33.2	–0.1	0.2	135
		–25.8	–1.1	1.9	121
3	S	–37.4	–0.4	0.7	86
		n.d.	n.d.	n.d.	138
		–28	–0.8	1.4	108
	P	–37.4	–0.4	0.7	218
		–54.8	–1.1	1.9	183
		–28.8	–1.1	1.9	224
		n.d.	n.d.	n.d.	201
		–25.8	–0.9	1.6	229
		–26.6	–1.7	2.9	242
		–23.5	–1.3	2.2	217
		–26	–0.5	0.9	230
	S	–27.3	–0.4	0.7	99
		n.d.	–0.3	0.5	116
		–23.2	–0.6	1.1	109

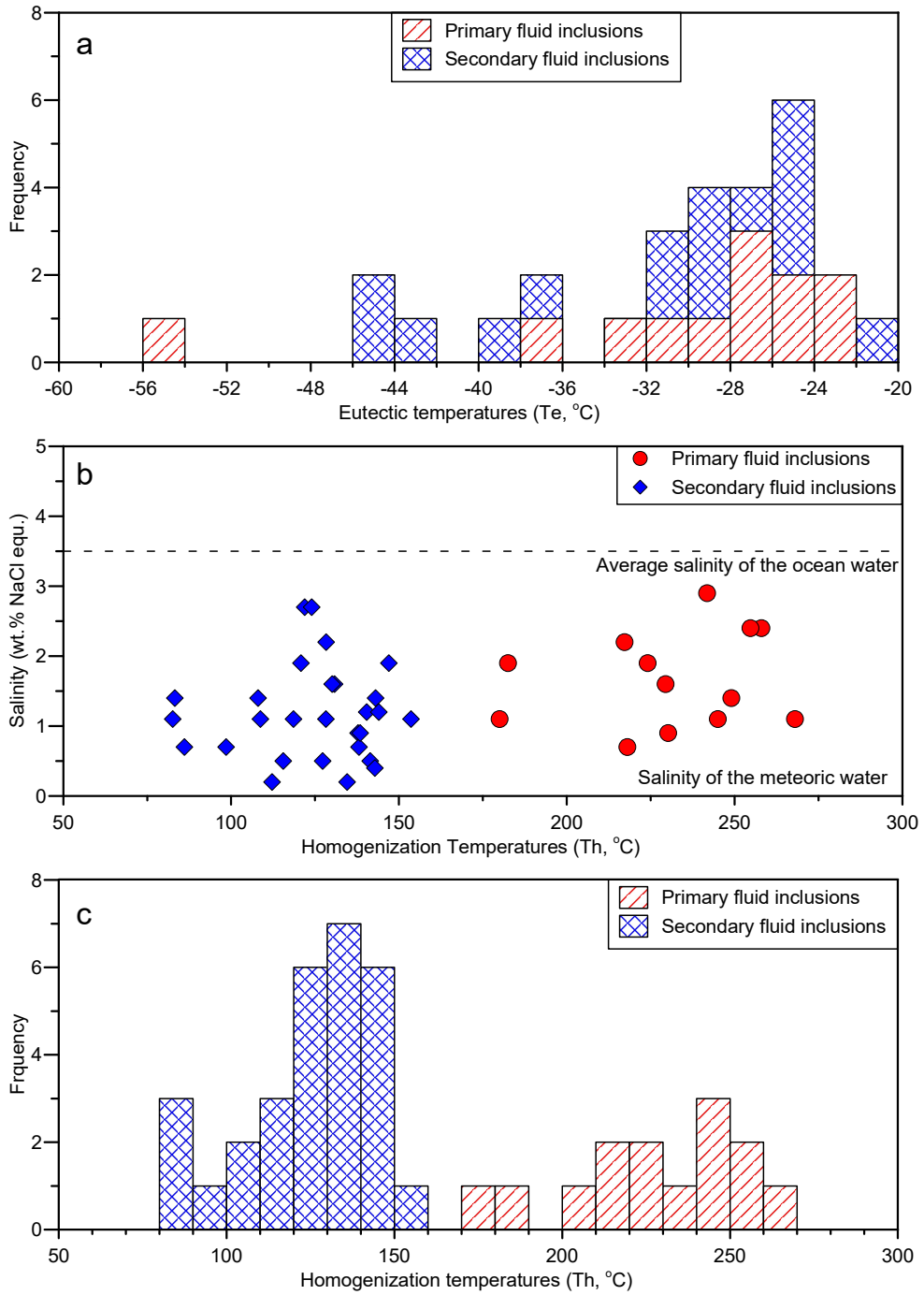

Figure 7. Eutectic temperature histogram (a), homogenization temperatures versus salinity values for the primary and secondary fluid inclusions (b), and homogenization temperature histogram (c) in the analcimes.

on the viscosity and flow rate of the lava (Polacci and Papale, 1997). Basaltic melts tend to exhibit low viscosities and high temperatures and consequently, have large chemical diffusivities. However, they also tend to have lower volatile contents compared to SiO_2-rich silicic melts, especially in the case of water. Vesiculation occurs in basaltic magma during slow ascents, decompression episodes, and in cooling columns near equilibrium (Best and Christiansen, 2001). Consequently, different types of vesiculation can occur in the same lava flow; for example, 2

separate vesicle regions were observed in the thick (<30 m) lava flows of the Colorado River (Figure 8). The first zone can be found near the top of the flow and contains vesicles that were formed and preserved during the eruption and subsequent lava flows. These vesicles are often found inside and beneath broken pieces of the flow that were created during the movement of the lava. The second vesiculated zone is located below this first zone, at approximately 40% of the total flow thickness. The vesicles in this zone were created by volatile-rich magma that was trapped within the magma during its ascent and subsequent cooling (Manga, 1996).

The Coppermine Formation consists of several lava flows with intercalated brecciation. Each lava flow is characterized by 2 zones: a soft and a hard zone (Smellie et al., 1984). The most likely explanation for the presence of these soft and hard zones is vesiculation, especially since both zones have similar mineralogical compositions. Specifically, differences in the volatile contents may have influenced the rheology of magmas in the softer zones. Densely vesiculated zones are easily altered/weathered compared to the less vesiculated zones. The thick lava flows of the Coppermine Formation exhibit 2 types of vesicular zones, similar to those of Colorado River basalts (Manga, 1996). Vesicles found in the brecciated zones at the top of the lava flows are smaller than the vesicles observed in the softer zones of the lava flows, which always occur beneath the brecciated zone. The harder zones, which generally occur between the brecciated and the softer zones, contain less than 10% vesicles, while the softer zones contain more than 30% vesicles. The size of the vesicles in these softer zones can reach up to several centimeters.

5.2. Secondary mineral assemblages and paragenetic sequences

The alteration of the basaltic rocks in the Coppermine Formation resulted in secondary mineral assemblages that described a multistage hydrothermal alteration process. The occurrence of secondary minerals in the vesicles was not homogeneous, and their associations may be significantly different on the hand sample scale. Nevertheless, 2 main paragenetic stages were identified in the vesicles of the Coppermine lava flows.

The first phase of the alteration involved the formation of clay and carbonate minerals. This paragenetic sequence was observed in vesicles less than 250 μm in size; these vesicles were characterized by central infillings composed of carbonates and lined by clay minerals (Figure 4). Larger vesicles were characterized by carbonate-filled voids with fragments of the clay mineral lines (Figure 4). In these vesicles, the formation of clay mineral lines

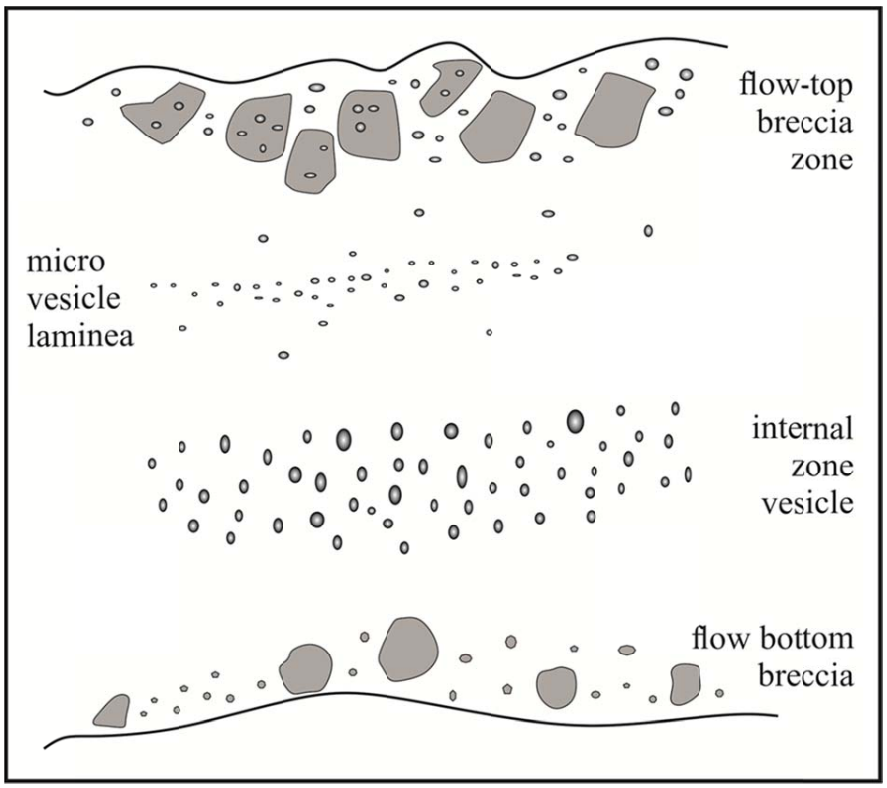

Figure 8. Vesiculation regions of the thick lava flow (modified from Manga, 1996).

on the walls of the cavities represents the first phase of alteration; precipitating carbonate solutions subsequently decomposed these.

Jeong et al. (2004) reported that the mixed chlorite/smectite layers in the sediments observed on the outer shelf of Livingstone Island, South Shetland Islands, were not formed by local pedogenic processes, they were instead derived from the erosion of hydrothermally altered volcanic rocks. Furthermore, data from the Icelandic geothermal fields showed that basaltic volcanic glass altered to mixed chlorite/smectite between 200 and 250 °C (Kristmannsdottir, 1985; Chipera and Apps, 2001; Figure 9). In light of these studies, the clay minerals found in the wall of the vesicles in the Coppermine Formation are likely to be chlorite/smectite mixed layer in composition and form the alteration of the host basaltic matrix by hydrothermal solutions.

Analcime and the accompanying zeolite minerals were formed in the second phase of alteration. Analcimes occurred in the cavities within the fragmented mixed clay mineral lines and carbonates, indicating that analcime and accompanying zeolite minerals were formed after the mixed clay mineral lines and carbonate minerals, and possibly even after the alteration of these fillings.

Data from the primary fluid inclusions within the analcime showed that it was formed from hydrothermal fluids at temperatures greater than 268 °C. This is in contrast to the temperatures of the hydrothermal solutions responsible for the formation of the analcime near the clay minerals (200–250 °C). Since the clay minerals formed earlier, at least 2 different scenarios can be considered for the origin of the hydrothermal solutions that resulted in the formation of the analcime. The first scenario involves the continuous heating of the hydrothermal fluids over time, which would have altered the basaltic matrix as it reached temperatures around 200–250 °C, allowing clay minerals to form in the walls of the cavities. As the temperature continues to increase (up to 250 °C), the alteration of plagioclase begins, with the resulting hydrothermal solution becoming increasingly rich in Si, Al, and Na and initiating the crystallization of the analcime. The temperature of the hydrothermal solution is likely to have reached its maximum value after this point. Secondary fluid inclusions in the analcime revealed that the temperature of the hydrothermal solution was decreasing. At this stage, the hydrothermal solutions would likely have been enriched in Ca, resulting in the formation of Ca–Na zeolites (e.g., stilbite, thomsonite) as the final crystallization products.

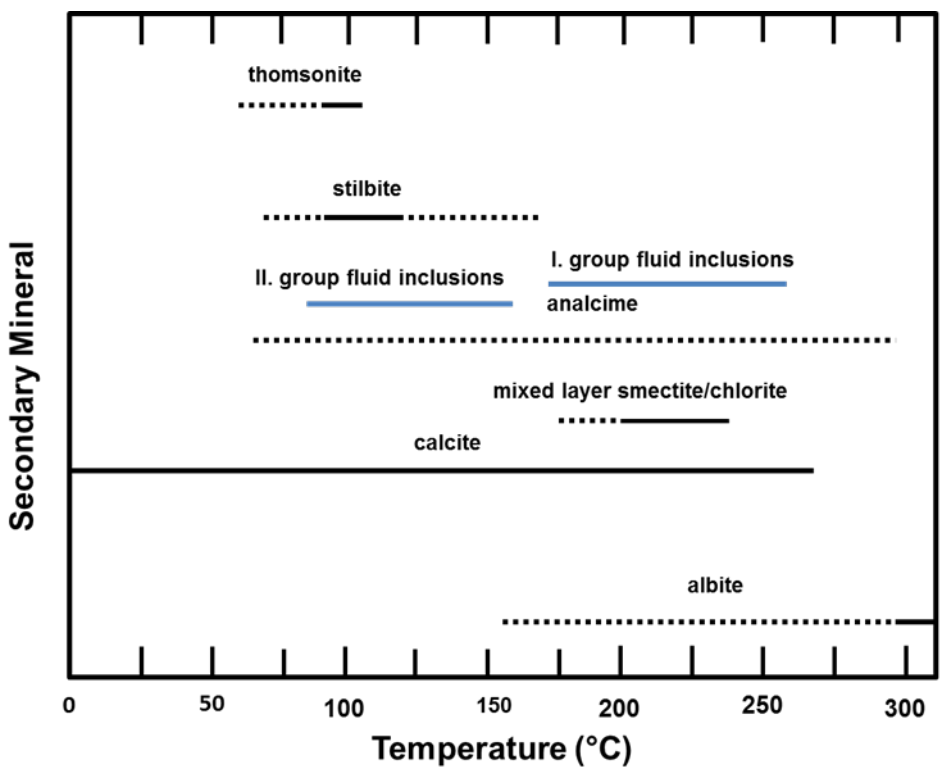

Figure 9. Comparison of the distributions of the secondary minerals as a function of temperature in the hydrothermally altered Icelandic basalts (from Chipera and Apps, 2001) and homogenization temperatures measured from the primary and secondary fluid inclusions of the analcimes.

The second scenario involves multiple stages of alteration during the formation of the South Shetland Islands, which involved a significant amount of intense magmatism between the Upper Cretaceous and the Pliocene. In particular, there have been several different ages reported for the young volcanic and plutonic rocks on the South Shetland Islands, such as Eocene Plutonism (Smellie et al., 1984), Oligocene volcanism (Birkenmajer, 1989), and Pliocene volcanism (Panczyk and Nawrocki, 2011). Smellie et al. (1984) reported that the age of the rocks of the Coppermine Formation ranged from 82–60 Ma. Over time, the volcanic rocks of the Coppermine Formation may have experienced several episodes of hydrothermal alteration. Assuming this to be the case, Type 1 infillings may correspond to precipitation of the hydrothermal solutions (the first stage of alteration), while Type 2 infillings may be products of in-situ weathering. Vesicle infillings, which would have disintegrated during weathering, would have been compacted by the introduction of secondary hydrothermal fluids, followed by the subsequent formation of analcime and zeolite crystals (Type 3 and 4 infillings). The petrography of the vesicles (such as traces of weathering on the clay minerals in the walls of the vesicles) suggests that the scenario involving multiple stages of alteration is more likely. Furthermore, the magmatic history of the South Shetland Islands supports this interpretation. However, the lack of data prevents further interpretations regarding the timing of these periods of alteration.

The Th of the primary fluid inclusions in the analcime crystals (180–268 °C) allowed for the estimation of the approximate formation temperature of the analcime crystals. The Th of the secondary fluid inclusions (83–154 °C) were interpreted to be the temperature as the hydrothermal fluids that were flowing through the cracks and fractures in the analcime; these fluids would have been the source of the accompanying zeolites, suggesting that these zeolites formed after the analcime crystallization. This formation sequence is consistent with the formation of the secondary minerals in the hydrothermally altered Icelandic basalts (Figure 9, Chipera and Apps, 2001).

In contrast, the Te of both types of fluid inclusions were relatively similar, ranging between –54 and –20.6 °C, suggesting that the analcime and accompanying zeolites were derived from NaCl-rich solutions that also contained a small amount of Mg- and Ca-salts. The salinity of both the primary and secondary fluid inclusions was also relatively similar, ranging between 0.2 and 2.9 wt.% NaCl equivalent. Consequently, there are concerns about whether analcime can form at such low NaCl concentrations. However, Slaby (1999) and Adamczyk and Bialecka (2005) showed experimentally that analcime precipitation could occur from a 0.1 M NaCl solution at temperatures above 120 °C; their experiments suggested that, at higher temperatures, analcime could precipitate from even lower NaCl concentrations.

The salinity of the fluid inclusions provides important information about the source of these hydrothermal fluids. For example, the salinity of fluid inclusions from ore-bearing hydrothermal systems directly related to magmatism is relatively high, reaching up to 90 wt.% NaCl equivalent (Wilkinson, 2001). In contrast, the salinity of systems that interact with ocean water would be relatively similar to that of seawater. Although the salinities of the examined fluid inclusions were relatively low, they were still well above that of fresh water (0.05 wt.% NaCl equivalent). Consequently, the salinities of the fluid inclusions suggest the mixing of meteoric waters and seawater at different rates. Since the timing of the hydrothermal alteration filling the vesicles cannot be constrained, it is difficult to pinpoint the exact contribution of glaciers to the meteoric waters that would have formed these hydrothermal fluids.

6. Conclusions

The Coppermine Formation is exposed on Robert Island, South Shetland Islands. This Upper Cretaceous formation consists of lava flows composed of bands of harder and softer material. The most crucial difference between these mineralogically similar zones is the abundance of vesicles, with the softer bands containing a greater abundance of vesicles. These vesicles are filled with a variety of minerals, including clay minerals, carbonates, analcimes, and zeolites. Fluid inclusion studies conducted on the analcime revealed that the temperature of the hydrothermal fluids from which the analcime precipitated was to close 268 °C. Additional analyses suggested that the vesicles were filled in at least 2 different alteration stages, with the clay and carbonate minerals being precipitated in the first stage of alteration. Following the weathering of the fillings formed during the first stage of alteration, the second stage of alteration occurred, resulting in the precipitation of analcime and zeolites from hydrothermal fluids. It is well-known that the South Shetland Islands experienced a significant amount of magmatic activity between the Cretaceous and the Pliocene. However, links between specific magmatic episodes and the different stages of hydrothermal alteration observed in the vesicle infillings could not be constrained. Nevertheless, it was found that the hydrothermal fluids from which the analcime and zeolites were derived were formed from the mixing of meteoric water and seawater in specific proportions.

Acknowledgments

This study was carried out under the generosity of the Presidency of the Republic of Türkiye, supported by the Ministry of Science, Industry, and Technology, and coordinated by the İstanbul Technical University Polar Research Center.

References

Adamczyk Z, Bialecka B (2005). Hydrothermal synthesis of zeolites from Polish coal fly ash. Polish Journal of Environmental Studies 14: 713-719.

Aydar E, Çubukçu E, Akın L (2019). Robert Adası-Coppermine Formasyonunun volkanolojik ve petrolojik incelenmesi, Güney Shetland Adaları, Batı Antaktika. 3, Kutup Bilimleri Çalıştayı Bildiri Özleri Kitabı, 17, 5-6 Eylül 2019, ODTÜ Kültür ve Kongre Merkezi, Ankara.

Bargar KE, Beeson MH (1985). Hydrothermal alteration in Research Drill Hole Y-3, Lower Geyser Basin, Yellowstone National Park, Wyoming. U.S. Geological Survey Professional Paper 1054-C: C1-C23. https://doi.org/10.3133/pp1054C

Bastías J, Chew D, Villanueva C, Riley T, Manfroi J et al. (2023). The South Shetland Islands, Antarctica: Lithostratigraphy and geological map. Frontiers in Earth Science 10: 1002760. https://doi.org/10.3389/feart.2022.1002760

Best M, Chirstiansen EH (2001). Igneous Petrology. Geological Magazine 139 (2): 233-238. https://doi.org/10.1017/S0016756802216507

Birkenmajer K (1989). A guide to tertiary geochronology of King George Island, West Antarctica. Polish Polar Research 10: 555-579.

Bodnar RJ (1993). Revised equation and table for determining the freezing point depression of H_2O-NaCl solutions. Geochimica et Cosmochimica Acta 57 (3): 683-684. https://doi.org/ 10.1016/0016-7037(93)90378-A

Boles JR, Coombs DS (1975). Mineral reactions in zeolitic Triassic tuff, Hokonui Hills, New Zealand. Geological Society of America Bulletin 86: 163-173.

Chipera SJ, Apps JA (2001). Geochemical stability of natural zeolites. Reviews in Mineralogy and Geochemistry 45 (1): 117-16. https://doi.org/10.2138/rmg.2001.45.3

Gall Q, Hyde R (1989) Analcime in lake and lake-margin sediments of the Carboniferous Rocky Brook Formation, western Newfoundland, Canada. Sedimentology 36: 875-887.

González Ferran O, Katsu Y (1970). Estudio integral del volcanismo cenozoico superior de las Islas Shetland del Sur, Antártica. Instituto Antártico Chileno. Ser. Científica 1-2: 123-174.

Haase KM, Beier C, Fretzdorff S, Smellie JL, Garbe-Schönberg D (2012). Magmatic evolution of the South Shetland Islands, Antarctica, and implications for continental crust formation. Contributions to Mineralogy and Petrology 163: 1103-1119. https://doi.org/10.1007/s00410-012-0719-7

Hein UF (1989). Microthermometry. Compact course and excercises, IGDL, University of Göttingen, pp. 52.

Hervé A (1965). Estudio geomorfológico y geológico en las Islas Greenwich y Robert. Shetland del Sur, Antártica. Tesis de Prueba. Departamento de Geología, Universidad de Chile 1-222.

Jeong GY, Yoon HI, Lee SY (2004). Chemistry and microstructures of clay particles in smectite-rich shelf sediments, South Shetland Islands, Antarctica. Marine Geology 209: 19-30. https://doi.org/10.1016/j.margeo.2004.05.027

Kamenov BK (2008). Multiepisodic dyke systems in Hurd Peninsula, Livingston Island, South Shetland Islands Volcanic Arc (Antarctica): petrological and geochemical implications for their magma evolution. Geochemistry, Mineralogy and Petrology 46: 103-142.

Keith TEC, Thompson JM, Mays RE (1983). Selective concentration of cesium in analcime during hydrothermal alteration, Yellowstone National Park, Wyoming. Geochimica et Cosmochimica Acta 47: 795-804. https://doi.org/10.1016/0016-7037(83)90113-8

Kraus S (2005). Magmatic dyke systems of the South Shetland Islands volcanic arc (West Antarctica): reflections of the geodynamic history. Als Dissertation eingereicht an der Fakultät für Geowissenschaften Ludwig-Maximilians-Universität München.

Kristmannsdottir H (1979). Alteration of basaltic rocks by hydrothermal activity at 100-300 °C. Developments in Sedimentology 27: 359-367. https://doi.org/10.1016/S0070-4571(08)70732-5

Kristmannsdottir H (1985). The role of clay minerals in geothermal energy research. Uppsala Symposium Clay Minerals-Modern Society.

Kuritani T, Yoshida T, Kimura J, Hirahara Y, Takahashi T (2014) Water content of primitive low-K tholeiitic basalt magma from Iwate Volcano, NE Japan arc: implications for differentiation mechanism of frontal-arc basalt magmas. Mineralogy and Petrology 108: 1-11. https://doi.org/10.1007/s00710-013-0278-2

Leat PT, Scarrow JH, Millar IL (1995). On the Antarctic Peninsula batholith. Geological Magazine 132: 399-412. https://doi.org/10.1017/S0016756800021464

Machado A, Lima EF, Chemale F, Morata D, Oteiza O et al. (2005) Geochemistry constraints of Mesozoic–Cenozoic calc-alkaline magmatism in the South Shetland arc, Antarctica. Journal of South American Earth Sciences 18: 407-425. https://doi.org/10.1016/j.jsames.2004.11.011

Manga M (1996). Waves of bubbles in basaltic magmas and lavas. Journal of Geophysical Research 101 (B8): 17457-17465. https://doi.org/ 10.1029/96JB01504

Panczyk M, Nawrocki J (2011). Pliocene age of the oldest basaltic rocks of Penguin Island (South Shetland Islands, northern Antarctic Peninsula). Geological Quarterly 55: 335-344.

Pearce TH (1970) The analcite-bearing volcanic rocks of the Crowsnest Formation, Alberta. Canadian Journal of Earth Sciences 7: 46-66. https://doi.org/10.1139/e70-004

Poblete F, Arriagada C, Roperch P, Astudillo N, Hervé F et al. (2011). Paleomagnetism and tectonics of the South Shetland Islands and the northern Antarctic Peninsula. Earth and Planetary Science Letters 302: 299-313. https://doi.org/10.1016/j.epsl.2010.12.01

Polacci M, Papale P (1997). The evolution of lava flows from ephemeral vents at Mount Etna: insights from vesicle distribution and morphological studies. Journal of Volcanology and Geothermal Research 76: 1-17. https://doi.org/10.1016/S0377-0273(96)00070-4

Putnis A, Putnis C, Ciriaco G (1994). The microtexture of analcime phenocrysts in igneous rocks. European Journal of Mineralogy 6: 627-632. https://doi.org/10.1127/ejm/6/5/0627

Roedder E (1984) Fluid inclusions as samples of ore fluids. In: Barnes HL (editor) Geochemistry of Hydrothermal Ore Deposits, 2nd ed. New York: Wiley Interscience, pp.684-737.

Shepherd TJ, Rankin AH, Alderton DHM (1985). A Practical Guide to Fluid Inclusion Studies. Glasgow (UK): Blackie and Son Limited, pp. 235.

Sheppard RA, Hay RL (2001) Formation of zeolites in open hydrologic systems. Reviews in Mineralogy and Geochemistry, Mineralogical Society of America, 45 (1): 261-276. https://doi.org/10.2138/rmg.2001.45.8

Slaby E (1999). Indicative significance of water environment in zeolitic structure – a study using experimentally grown cancrinite and analcime. Acta Geologica Polonica 49 (1): 25-65.

Smellie JL, Pankhurst R., Thomson MRA, Davies RES (1984). The geology of the South Shetland Islands, VI. Stratigraphy, geochemistry and evolution. British Antarctic Survey Scientific Report, 87: 85.

Stein DJ, Spera FJ (1992). Rheology and microstructure of magmatic emulsions: theory and experiments. Journal of Volcanology and Geothermal Research 49 (1-2): 157-174. https://doi.org/10.1016/0377-0273(92)90011-2

Stone DH (1994). Dynamics of deformation and break up in viscous fluids. Annual Review of Fluid Mechanics 26: 65-102. https://doi.org/10.1146/annurev.fl.26.010194.000433

Triana JM, Herrera JF, Rios AC, Castellanos OM, Heano JA et al. (2012). Natural zeolite filling amygdalas and veins in basalt from the Tertiary Igneous Province on Isle Skye, Scotland. Earth Sciences Research Journal 16 (1): 41-53.

Ushioda M, Takahashi E, Hamada M, Suzuki T (2014). Water content in arc basaltic magma in the Northeast Japan and Izu arcs: an estimate from Ca/Na partitioning between plagioclase and melt. Earth, Planets and Space 66: 127-137. https://doi.org/10.1186/1880-5981-66-127

Villanueva C (2021). Caracterización geocronológica, petrográfica y Geoquímica del volcanismo de arco durante el Cretácico superior en la Península Coppermine, Isla Robert, Antártica: Migración del magmatismo versus Arco continuo. Santiago. PhD Thesis, Departamento de Geología, Universidad Santo Tomás.

Weisenberger T, Selbekk RS (2010). Multi-stage zeolite facies mineralization in the Hvalfjördur area, Iceland. International Journal of Earth Sciences 98: 985-999. https://doi.org/10.1007/s00531-007-0296-6

Wilkinson JJ (2001). Fluid inclusions in hydrothermal ore deposits. Lithos 55: 229-272. https://doi.org/10.1016/S0024-4937(00)00047-5